

## ESTIMATION OF MAXIMUM AND MINIMUM INDUCTANCE OF 6/4 SWITCHED RELUCTANCE MACHINE

Eng. Hassan mahmoud \*, Prof. M. M. El-Shamoty \*\*, Dr. Ahmed farahat \*\*,  
Dr. Mohammed El-Sersawi \*\*\*

*\*Electrical Engineer, Talkha power station*

*\*\* Electrical & Machine Dept., Faculty of Eng., Mansoura University*

*\*\*\* Major General Doctor, Egyptian Armed forces*

### Abstract

Switched Reluctance Machines (SRMs) are receiving significant attention from industries in the last decade. SRMs are rather inexpensive, reliable and weigh less than other machines of comparable power outputs. The goal of this paper is to investigate how to estimate the maximum and minimum inductance of the switched reluctance machine by the flux map method.

ازداد الاهتمام بمحركات المعاوقة للتيار المقطع خلال الاعوام الاخيرة نتيجة للميزات التي يتمتع بها هذا النوع من المحركات مما يجعله يستخدم في كثير من التطبيقات الصناعية . والهدف الرئيسي لهذا البحث هو كيفية حساب اكبر واقل قيمة ممانعة لآلة الممانعة المغناطيسية حيث أن تلك القيم تعد من أهم البارامترات التي تشترك في تصميم الآلة. والطريقة المستخدمة في حساب تلك القيم تستخدم التوزيع الإفتراضى للفيض المغناطيسى داخل الآلة.

### 1-Introduction

The reluctance machine is an electric machine in which torque is produced by the tendency of its moveable part to move to a position where the inductance of the excited winding is maximized [1, 2]. The origin of the reluctance machine can be traced back to 1842, but the “reinvention” has been possibly due to the advent of inexpensive, high-power switching devices [9]. The reluctance machine is a type of synchronous machine. It has wound field coils of a DC motor for its stator windings and has no coils or magnets on its rotor [3, 4]. The basic purpose of this paper is how to estimate the maximum and minimum inductance of the switched reluctance machine.

### 2: Motor specification.

- 1: Number of stator poles  $N_s = 6$
- 2: Number of rotor poles  $N_r = 4$
- 3: Stator pole arc  $\alpha_s = 30^\circ$  mech
- 4: Rotor pole arc  $\alpha_r = 33^\circ$  mech
- 5: Air gap length  $g = 0.25$  [mm]
- 6: Air gap length of the interpolar space  $g_i = 27$  [mm]
- 7: Rotor diameter  $d = 88.4$  [mm]
- 8: Stator outside diameter  $d_o = 165.1$  [mm]
- 9: Back iron width  $c = 88.1$  [mm]
- 10: Core length  $l = 108$  [mm]
- 11: Number of turn per phase  $N = 1150$  turn  
 $P = 1.1$  kw.

**3: Estimation of the minimum inductance [5].**

Figure 1 shows a sketch of the field pattern of the magnetic configuration corresponding to the minimum inductance position. The figure represents typical dimensional proportions of the magnetic configuration of a switched reluctance machine. The field map in the air space inside the machine may be divided into six paths [5, 6].

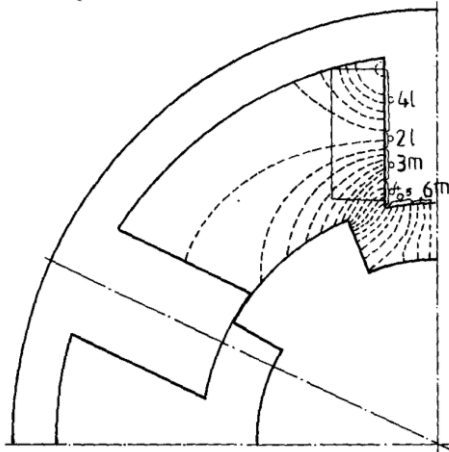


**Fig. 1:** Sketch of the field pattern in minimum inductance position.

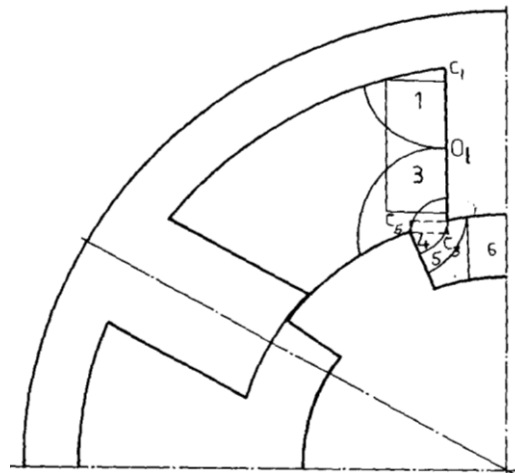


**Fig. 2:** Approximated flux paths.

(Path 1ℓ) consists of the field lines which lead from the excited stator pole side to the stator back of core. These Field lines consist of concentric circular arcs with the centre at the point C<sub>1</sub> as in Figure 2.

(Path 2ℓ) consists of field lines which lead from the stator pole side to the adjacent pole. These Field lines will be ignored.

(Path 3r), consists of the Field lines which lead from the stator pole side to the rotor pole surface. These Field lines consist of the concentric circular arcs with the center at the point C<sub>3</sub>.

(Path 4), consists of lines which lead from the stator pole side to the rotor pole side [7].

(Path 5), consists of lines which lead from the stator pole face to the rotor pole side. These Field lines consist of concentric circular arcs with the center at the point C<sub>5</sub>.

(Path 6), consists of the lines which lead from the stator pole face to the rotor interpolar surface. These Field lines consist of parallel straight line segments.

Since the magnetic configuration in the minimum inductance position is symmetrical with respect to the pole axis and with respect to the axis perpendicular to it, then flux-linkage of one pole coil is:

$$\Psi = 2(\Psi_1 + \Psi_3 + \Psi_4 + \Psi_5 + \Psi_6) \quad (1)$$

Where  $\Psi_1, \Psi_3, \Psi_4, \Psi_5, \Psi_6$  are flux-linkages of the paths 1, 3, 4, 5, 6 respectively. The total inductance of one phase is:

$$\begin{aligned} L_0 &= \frac{4}{i} (\Psi_1 + \Psi_3 + \Psi_4 + \Psi_5 + \Psi_6) \\ &= 4 (L_1 + L_3 + L_4 + L_5 + L_6) \\ &= N^2 \mu_0 \ell_F (P_1 + P_3 + P_4 + P_5 + P_6) \\ &= N^2 \mu_0 \ell P_0(3) \end{aligned} \quad (2)$$

Where,

$$P_j = L_j / [\mu_0 \ell_F (\frac{N}{2})^2],$$

(j = 1, 3, 4, 5, 6)

$\ell_F$ : the effective core length,

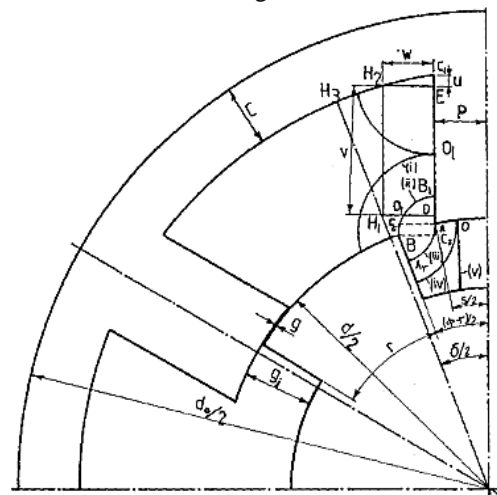


**Fig (3)** Dimensional description of magnetic configuration

$P_0 = \sum_{j=1}^6 P_j$  is the total normalized equivalent minimum permeance.

The magnetic configuration is described by the following set of parameters as shown in figure 3. Number of stator poles  $N_s$ , Number of rotor poles  $N_r$ , Stator pole arc  $s$ , Rotor pole arc  $r$ , Air-gap length  $g$ , Rotor diameter  $d$ , Back iron width  $c$ , Air-gap length of rotor interpolar space  $g_i$ , Core length

$\ell$ , Stator outside diameter  $d_0$ , Number of turns per phases N [8, 9].

Using the above parameters, the remaining angles and dimensions in figure 3 may be determined [5, 6 and 7].

$$\text{Rotor pole pitch} = \Phi = \frac{2\pi}{N_r} \quad (3)$$

$$\text{Stator pole pitch} = \delta = \frac{2\pi}{N_s} \quad (4)$$

$$\text{Angle H1C1E} = \gamma = \frac{\pi}{2} - \frac{\delta}{4} \quad (5)$$

$$\text{Stator pole width} = 2p = 2\left(\frac{d_1}{2} + g\right) \sin \frac{\delta}{2} \quad (6)$$

$$\text{Coil width } w = \left(\frac{d_2}{2} + g\right) \tan \frac{\delta}{2} - p \quad (7)$$

$$\text{Coil high} = v \approx \left[ \frac{d_0}{2} - c - \frac{w}{2} \right] \frac{1}{\cos \frac{\delta}{2}} \quad (8)$$

The lengths between marked points are:

$$h = C_3 B_1 \approx \frac{d}{2} \sin \frac{\phi-r}{2} - p \quad (9)$$

$$C_3 D = y = \left(\frac{d}{2} + g\right) - \frac{d}{2} \cos \frac{\phi-r}{2} \quad (10)$$

$$b = BC_5 = \left(\frac{d}{2} + g\right) \cos \frac{\delta}{2} - \frac{d}{2} \cos \frac{\phi-r}{2} \quad (11)$$

$$q = E O_t = \frac{v}{2} \quad (12)$$

$$u = C_1 E = \frac{w}{\tan \gamma} \quad (13)$$

$$m = C_1 O_t = u + q \quad (14)$$

$n = C_3 O_t = y + q$   
Normalizing the dimensions with respect to the outside stator diameter gives:

$$G = \frac{g}{d_0}, G_i = \frac{g_i}{d_0}, D = \frac{d}{d_0}, C = \frac{c}{d_0}, L_F = \frac{\ell_F}{d_0}$$

Then the normalized values  $p, w, v, Y, H, B, Q, U, M, N$  are :

$$P = \left(\frac{D}{2} + G\right) \sin \frac{\delta}{2} \quad (15)$$

$$W = \left(\frac{D}{2} + G\right) \tan \frac{\delta}{2} - p \quad (16)$$

$$V = \left(\frac{1}{2} - C - \frac{D+G}{\cos \frac{\delta}{2}}\right) \frac{1}{\cos \frac{\delta}{2}} \quad (17)$$

$$Y = \frac{D}{2} + G - \frac{D}{2} \cos \frac{\phi-r}{2} \quad (18)$$

$$H = \frac{D}{2} \sin \frac{\phi-r}{2} - pB = \left(\frac{D}{2} + G\right) \cos \frac{\delta}{2} - \frac{D}{2} \cos \frac{\phi-r}{2} \quad (19)$$

$$Q = \frac{V}{2} \quad (20)$$

$$U = \frac{W}{\tan \gamma} \quad (21)$$

$$N = Y + Q, M = U + Q \quad (22)$$

### 3.1. Calculation of minimum inductance components:

a) Component  $L_1$ .

$$L_1 = \frac{\int_{(\phi)}^{(m)} d\Psi_x}{i} = \mu_0 \ell_F \left(\frac{N}{2}\right)^2 \frac{\gamma m^4}{4w^2 (2V+w)^2} \quad (23)$$

$$P_1 = \frac{L_1}{\mu_0 \ell_F \left(\frac{N}{2}\right)^2} = \frac{\gamma m^4}{4w^2 (2V+w)^2} \quad (24)$$

$$P_1 = 0.054 = 0.024 P_0 \quad (25)$$

b) Component  $L_3$ .

$$L_3 = \frac{\int_{(h)}^{(n)} d\Psi_x}{i} = \frac{2}{\pi} \left\{ \ln \frac{n}{h} + \frac{2(n-h)y}{wv} - \frac{(n^2-h^2)}{4(wv)^2} (\pi wv - 2y^2) - \frac{(n^2-h^2)y\pi}{6(wv)^2} + \frac{(n^4-h^4)\pi^2}{64(wv)^2} \right\} \mu_0 \ell_F \left(\frac{N}{2}\right)^2 \quad (26)$$

$$P_3 = \frac{L_3}{\mu_0 \ell_F \left(\frac{N}{2}\right)^2} = \frac{2}{\pi} \left\{ \ln \frac{N}{H} + \frac{2(N-H)Y}{wv} - \frac{(N^2-H^2)}{4(wv)^2} (\pi wv - 2Y^2) - \frac{(N^2-H^2)Y\pi}{6(wv)^2} + \frac{(N^4-H^4)\pi^2}{64(wv)^2} \right\} \quad (27)$$

$$P_3 = 0.458 = 0.211 P_0 \quad (28)$$

c) Component  $L_4$ :

$$L_4 = \mu_0 \ell_F \left(\frac{N}{2}\right)^2 \frac{2}{\phi-r} \ln \frac{2 \tan(\phi-r) + \pi - 2(\phi-r)}{2 \tan(\phi-r) + \pi - 2(\phi-r)} \quad (29)$$

$$P_4 = \frac{L_4}{\mu_0 \ell_F \left(\frac{N}{2}\right)^2} = \frac{2}{\phi-r} \ln \frac{2 \tan(\phi-r) + \pi - 2(\phi-r)}{2 \tan(\phi-r) + \pi - 2(\phi-r)} \quad (30)$$

$$P_4 = 0.557 = 0.257 P_0 \quad (31)$$

d) Components  $L_5$  and  $L_6$ :

$$L_5 = \mu_0 \ell_F \left(\frac{N}{2}\right)^2 \frac{2}{\pi - (\phi-r)} \ln \frac{2g_i}{h[\pi - (\phi-r)]} \quad (32)$$

$$P_5 = \frac{L_5}{\mu_0 \ell_F \left(\frac{N}{2}\right)^2} = \frac{2}{\pi - (\phi-r)} \ln \frac{2g_i}{H[\pi - (\phi-r)]} \quad (33)$$

$$P_5 = 0.474 = 0.218 P_0 \quad (34)$$

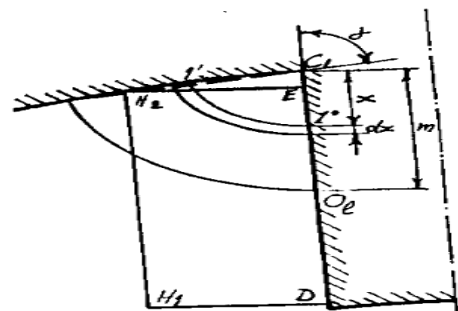


Fig (4) Detail with flux path 1

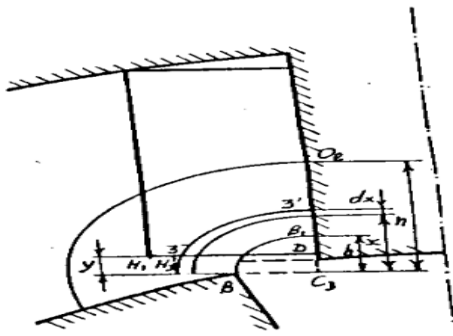


Fig (5) Detail with flux path 3

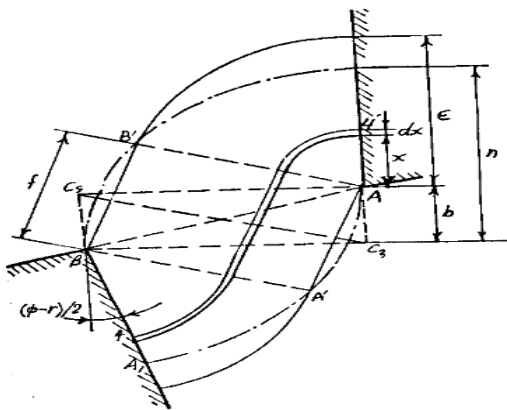


Fig (6) Detail with flux path 4.

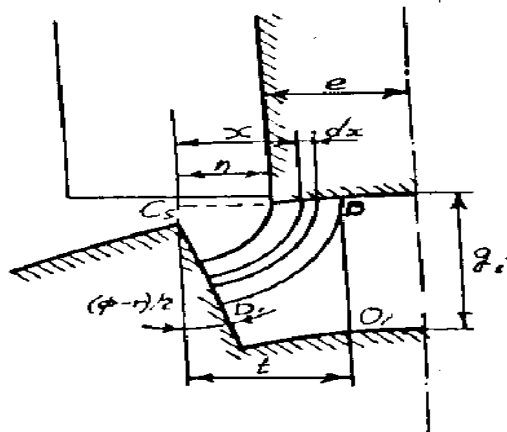


Fig (7) Detail with flux paths 5 and 6.

$$L_6 = \mu_0 \ell_F \left(\frac{N}{2}\right)^2 \left[ \frac{p+h}{g_i} - \frac{2}{\pi-(\theta-r)} \right] \quad (35)$$

$$P_6 = \frac{L_6}{\mu_0 \ell_F \left(\frac{N}{2}\right)^2} = \frac{p+h}{g_i} - \frac{2}{\pi-(\theta-r)} \quad (36)$$

$$P_6 = 0.320 = 0.147 P_0. \quad (37)$$

#### 4: Estimation of the maximum inductance using B-H curve [5].

In the maximum inductance position the MMF drop in the iron considerable, even in the case when the iron is not saturated, in comparison with MMF drop in the air- gap (the air- gap length is very small compared with the rotor diameters, typically  $g$  is about  $.005d$ ). When the iron becomes saturated the MMF drop in the iron increases nonlinearly and may exceed the MMF drop in the air- gap. Therefore the MMF drop in the iron and the nonlinearity of B-H curve of iron must be taken into account for estimation of the maximum inductance. To estimate the maximum inductance  $L_i$  by a simple analytical method the following assumption are made:

- 1: When a phase winding is excited the magnetic circuit is treated as a simple '2-pole' pattern Fig (8);
- 2: There is no flux leakage, ie all flux passes from the stator to the rotor and back;
- 3: the flux is linked with all turns;
- 4: The flux is uniformly distributed in the cross-section normal to the field lines.

In the maximum inductance position the field pattern is symmetrical about the axis of excited phase and therefore only one half of the magnetic circuit, which carries one half of the total flux, need be considered. Further than simplification is to split this half of the magnetic circuit into the following parts connected in the series:

- 1: Two stator poles (subscript's') with Cross-section:

$$a_s = \frac{d}{2} \left( \sin \frac{\alpha}{2} \right) l = 496.2 \text{ [mm}^2] \quad (38)$$

$$\text{Length: } l_s = 2 \left( \frac{d}{2} - c - \frac{r}{2} - g \right) = 44.9 \text{ [mm]} \quad (39)$$

- 2: Two air- gap (subscript 'g') with Cross-section\*:  $a_g = \left[ 0.5 \left( \frac{d}{2} + g \right) s + (1 - \sigma) i \right] l = 531.1 \text{ [mm}^2]$  (40)

$$\text{Where, } i = 0.5 \frac{d}{2} (r - s) \quad (41)$$

$$\sigma = \frac{2}{\pi} \left[ \arctan \left( \frac{i}{g} \right) - \frac{g}{2i} \ln \left( 1 + \left( \frac{i}{g} \right)^2 \right) \right] \quad (42)$$

$$\text{Length: } l_g = 2g = 0.508 \text{ [mm]}$$

- 3: Two rotor poles (subscript 'r') with Cross- section\*\*:  $a_r = a_g = 531.1 \text{ [mm}^2]$

$$\text{Length: } l_r = 2g_i = 18 \text{ [mm]}$$

- 4: Rotor body (subscript 'b') with

$$\text{Cross-section } a_b = \left( \frac{d}{2} - g_i \right) l = 2172 \text{ [mm}^2] \quad (43)$$

$$\text{Length: } l_b = 0.5 \left( \frac{d}{2} - g_i \right) \pi = 44.8 \text{ [mm]} \quad (44)$$

- 5: Stator yoke (subscript 'y') with Cross- section:  $a_y = cl = 746.8 \text{ [mm}^2]$  (45)

$$\text{Length: } l_y = 0.5(d_o - c)\pi = 204.5 \text{ [mm]} \quad (46)$$

The MMF equation is

$$Ni = \frac{B_g}{\mu_0} l_g + H_s l_s + H_r l_r + H_b l_b + H_y l_y \quad (47)$$

Having given the value of flux-linkage, the value of flux densities  $B_g$ ,  $B_s$ ,  $B_r$ ,  $B_b$  and  $B_y$  can be calculated  $B = \frac{\Psi}{Na}$  and using B- H curve of the appropriate steel the values for  $H_s$ ,  $H_r$ ,  $H_b$  and  $H_y$  can be found using the mmf equation the value of current corresponding to a given value of flux linkage can be found and hence the maximum inductance is  $L_i = \Psi / i$ . The normalized equivalent maximum permeance is given by:

$$P_i = \frac{L_i}{\mu_0 N^2} \quad (48)$$

Fig (9) shows the  $\Psi$ -i curve at the maximum inductance position which is obtained by measurement, 2-dimensional numerical field analysis and by using the above method. (The B-H curve in Fig (9) has been obtained by measurements on a steroidal iron specimen.) Bearing in mind that the above simple analytical method treats a very simplified field pattern, the error which is within 5% (in terms of inductance) is not so bad. In non saturated region of the  $\Psi$ -i the estimated and measured results are very close. Extremely good agreement between the measured  $\Psi$ -i curve of maximum inductance position and the one obtained by using 2-dimensional numerical field analysis shows that the fringe flux at the ends of core in maximum inductance position is negligible compared with the flux within machine [10, 11].

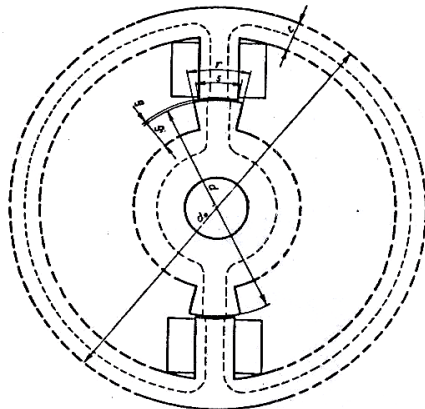


Fig (8) Simple "2-pole "pattern

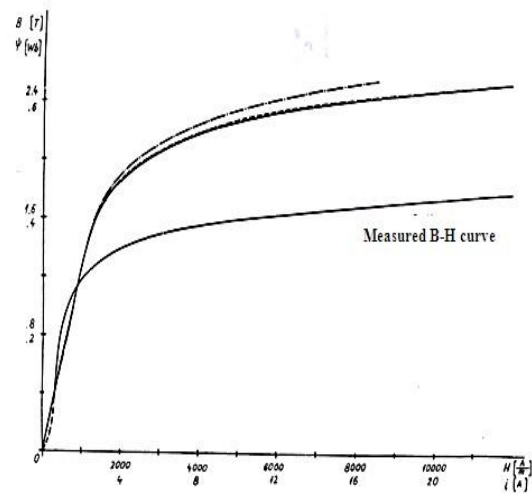


Figure 9 B-H curve and  $\Psi$ -i curve in maximum inductance position  
 — measured  
 ----- computed by numerical field solution  
 -.-.-.- estimated by simple analytical method

Table 1  
List of Symbol

Symbol	Description
$N_s$	Number of stator poles
$N_r$	Number of rotor poles
s	Stator pole arc
r	Rotor pole arc
$V_i$	applied voltage
I	Instantaneous current
$\theta$	Angle description the rotor angle
$\Psi$	Flux $\square$ linkage
$\omega$	Rotor speed
V	Applied voltage
E	The delay angle. $= \frac{\pi}{q}$
$\frac{d\theta}{dt}$	instantaneous speed
$\Phi$	Rotor pole pitch
$l$	Core length
C	Back iron width
$l_f$	The effective core length
$P_0$	total normalized equivalent minimum permeance
$\Delta$	Stator pole pitch
P	Half stator pole width
W	Coil width
$H_x$	Field on the elementary flux path
$d\Psi_x$	Elementary flux-linkage
$\alpha$	Ratio of maximum to minimum inductance
$g_f$	uniform air-gap
$\sigma$	Carter's coefficient

## 5: Conclusion

A method for the simple analytical estimation of the minimum and maximum inductance has been given. The estimation is valid even in the case where the realistic situation in the iron (saturation) is considered. The method of estimation of the minimum inductance is based on the assumption that the field lines consist of circular arcs and straight line segment. The distribution of the winding is allowed for. The estimated value of the minimum inductance, when the fringe flux at the ends of core is excluded, agrees very well with the result obtained by 2-dimensional numerical field solution (using the boundary- integral method, the difference is 2.7% ). An allowance base on a rough approximation for the fringe flux at the ends of the core has been made. The estimated value of the total minimum inductance is 14% lower than measured value for  $l/d = 1.0$  .In the maximum inductance positions the machine is treated as a simple 2- pole pattern and it is assumed that the flux linked with all turns and there is no flux leakage. The B-H curve of the iron is used in calculating the maximum inductance. The difference between measured and estimated values of the maximum inductance within 5% in the saturated region of the  $\Psi - i$  curve and is insignificant in the no saturated region.

## REFERENCES

- [1] Jaewook Lee, "STRUCTURAL DESIGN OPTIMIZATION OF ELECTRIC MOTORS TO IMPROVE TORQUE PERFORMANCE", Ph. D. Thesis, Dept. of Mechanical Engineering in The University of Michigan 2010.
- [2] T.J.E. Miller, "Switched reluctance motors and their control", Hillsboro, OH :MagnaPhysics Pub.; Oxford: Clarendon Press, 1993.
- [3] W. Lu, A. Keyhani, A. Fardoun, "Neural Network-Based Modeling and Parameter Identification of Switched Reluctance Motors", IEEE Transactions on Energy Conversion, Vol. 18, No. 2, June 2003.
- [4] F. Bokose, L. Vandeveld, J. Gyselinck, and J. Melkbeek, "DESIGN OF SWITCHED RELUCTANCE MOTORS BY USING NUMERICAL TECHNIQUES", Proceedings of Power Electronics, Electrical Drives, Automation & Motion, pp. c5-45-c5-50, Ravello (Italy), June, 2002.
- [5] M. El-Sersawy, "Analysis and experimental investigations of switched reluctance machines", Ph. D. Thesis, Dept. of Electrical power & Machine, Faculty of Engineering, El Mansoura University, Egypt, 1989.
- [6] R. Krishnan " Switched Reluctance Motor Drives: Modeling, Simulation, Analysis, Design, and Applications", IEEE the Bradley Department of Electrical and Computer Engineering, 2001.
- [7] Cheewoo Lee, R. Krishnan and N. S. Lobo, " Novel Two-Phase Switched Reluctance Machine Using Common-Pole E-Core Structure: Concept, Analysis, and Experimental Verification", IEEE TRANSACTIONS ON INDUSTRY APPLICATIONS, VOL. 45, NO. 2, MARCH/APRIL 2009.
- [8] Praveen Vijayraghavan, " Design of Switched Reluctance Motors and Development of a Universal Controller for Switched Reluctance and Permanent Magnet Brushless DC Motor Drives", DOCTOR OF PHILOSOPHY IN ELECTRICAL ENGINEERING, November 15, 2001.
- [9] Saphir Faid, Patrick Debal, and Steven Bervoets, " Development of a Switched Reluctance Motor for Automotive Traction Applications", © EVS-25 Shenzhen, China, Nov. 5-9, 2010.
- [10] Subhadra Devi Ganti, " ANALYSIS OF PERFORMANCE OF SINGLEPHASERELUCTANCE LINEAR MOTOR", Master of Science in Electrical Engineering, Faculty of the Louisiana State University, Hyderabad, India, May, 2005
- [11] James M. Kokernak and David A. Torrey, " Magnetic Circuit Model for the Mutually Coupled Switched-Reluctance Machine", IEEE TRANSACTIONS ON MAGNETICS, VOL. 36, NO. 2, MARCH 2000.